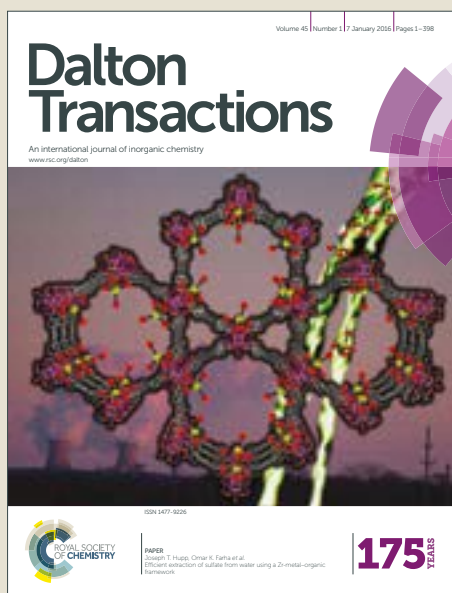


Dalton Transactions

Accepted Manuscript



This article can be cited before page numbers have been issued, to do this please use: M. L. Perrone, E. Salvadeo, E. Lo Presti, L. Pasotti, E. Monzani, L. Santagostini and L. Casella, *Dalton Trans.*, 2017, DOI: 10.1039/C7DT00147A.



This is an Accepted Manuscript, which has been through the Royal Society of Chemistry peer review process and has been accepted for publication.

Accepted Manuscripts are published online shortly after acceptance, before technical editing, formatting and proof reading. Using this free service, authors can make their results available to the community, in citable form, before we publish the edited article. We will replace this Accepted Manuscript with the edited and formatted Advance Article as soon as it is available.

You can find more information about Accepted Manuscripts in the [author guidelines](#).

Please note that technical editing may introduce minor changes to the text and/or graphics, which may alter content. The journal's standard [Terms & Conditions](#) and the ethical guidelines, outlined in our [author and reviewer resource centre](#), still apply. In no event shall the Royal Society of Chemistry be held responsible for any errors or omissions in this Accepted Manuscript or any consequences arising from the use of any information it contains.



Journal Name

ARTICLE

A dinuclear biomimetic Cu complex derived from L-histidine: Synthesis and stereoselective oxidations

Maria L. Perrone,^a Elena Salvadeo,^a Eliana Lo Presti,^a Luca Pasotti,^{a,b} Enrico Monzani,^a Laura Santagostini,^c Luigi Casella^{*a}

^aDipartimento di Chimica, Università di Pavia, Via Taramelli 12, 27100 Pavia, Italy

^bNoxamet Srl, Dipartimento di Chimica, Università di Pavia, 27100 Pavia, Italy

^cDipartimento di Chimica, Università di Milano, 20133 Milano, Italy

Received 00th January 20xx,
Accepted 00th January 20xx

DOI: 10.1039/x0xx00000x

www.rsc.org/

The dinuclear copper(II) complex derived from the chiral N₆ ligand (2*S*,2'*S*)-*N,N'*-(ethane-1,2-diyl)bis(2-((1-methyl-1*H*-imidazol-4-ylmethyl)-amino)-3-(1-trityl-1*H*-imidazol-4-yl)propanamide) (EHI) was synthesized and studied as catalyst in stereoselective oxidation reactions. The ligand contains two sets of tridentate binding units, each of them giving rise to a coordination set consisting in a pair of 5- and 6-membered chelate rings, connected by an ethanediamide linker. Stereoselectivity effects were studied in the oxidations of a series of chiral L/D biogenic catechols and the couple of L/D-tyrosine methyl esters, in this case as their phenolate salts. The oxidation of β-naphthol has also been studied as a model monooxygenase reaction. The catechol oxidation was investigated in a range of substrate concentrations at slightly acidic pH and exhibited a marked dependence on the concentration of [Cu₂EHI]⁴⁺ complex. This behavior has been interpreted in terms of an equilibrium between a monomeric and a dimeric form of the catalyst. Binding studies of L- and D-tyrosine were performed as a support for the interpretation of the stereoselectivity effects observed in the reactions. In general, [Cu₂EHI]⁴⁺ exhibits a binding preference for the L- rather than the D-enantiomer of the substrates, but it appears that in the catecholase reaction the oxidation of the D-isomer occurs at a faster rate than for the L counterpart. The same type of enantio-discriminating behavior is observed in the oxidation of L/D-tyrosine methyl esters. In this case the reaction produces a complex mixture of products; a main product consisting of a trimeric compound, likely formed by radical coupling reactions, has been isolated and characterized. The oxidation of β-naphthol yields an addition product of the expected quinone but labeling experiments with 18-O₂ show no oxygen incorporation into the product, confirming that the oxidation likely proceeds through a radical mechanism.

INTRODUCTION

The dicopper enzyme tyrosinase continues to be an important source of inspiration for biomimetic chemists interested in developing effective catalysts for oxygenation reactions.¹⁻⁴ Indeed, recent reports described the first examples of catalytic phenol hydroxylation^{5,6} and sulfoxidation⁷ by dinuclear copper complexes in the presence of dioxygen. A wealth of spectroscopic and structural studies on dicopper biomimetic model compounds of tyrosinase have shown that three types of copper-dioxygen intermediates are competent to perform

oxygen transfer reactions to the substrates:^{1-3,8,9} the μ-η²:η²-peroxodicopper(II), bis(μ-oxo)dicopper(III) or trans-μ-η¹:η¹-peroxodicopper(II) species. The currently available evidence on tyrosinase indicates that the enzyme performs the phenol hydroxylation through a μ-η²:η²-peroxodicopper(II) intermediate.⁸ An important development for synthetic applications of biomimetic tyrosinase models would be the possibility to perform catalytic stereoselective oxidations. The potential of copper salts, or simple complexes in mediating stereoselective reactions, in the presence of chiral additives, is well known and steadily expanding in synthetic organic chemistry.⁹ However, the nature of the active species and its nuclearity in these reactions is usually unknown, and therefore developing well characterized, biomimetic systems capable of promoting asymmetric reactions will open the field to the possibility to design chiral complexes for specific applications. We have been interested for some time in the synthesis of polydentate nitrogen ligands to obtain chiral dinuclear and

^a Dipartimento di Chimica, Università di Pavia, Via Taramelli 12, 27100 Pavia, Italy

^b Noxamet Srl, Dipartimento di Chimica, Università di Pavia, 27100 Pavia, Italy

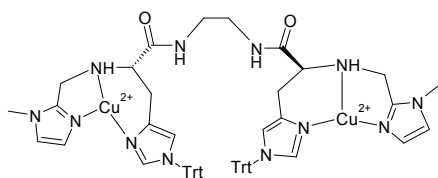
^c Dipartimento di Chimica, Università di Milano, 20133 Milano, Italy

† Footnotes relating to the title and/or authors should appear here.

Electronic Supplementary Information (ESI) available: Derivation of the kinetic equations, Uv-Vis and NMR spectra, kinetic plots, and characterization analysis of different products. See DOI: 10.1039/x0xx00000x

ARTICLE

trinuclear complexes.¹⁰⁻¹² These ligands typically contained a set of eight donor nitrogens and were designed to host three copper(II) centers, although for comparison purposes also the corresponding dinuclear analogues were in parallel developed. The reason for introducing a third metal center, in addition to the pair of copper centers acting as dioxygen activation site, was to exploit the binding properties of this center for anchoring the substrate close to the catalytic unit. Indeed, the trinuclear complexes generally exhibited better chiral discrimination properties with respect to the corresponding dinuclear counterparts. However, the synthetic routes to such chiral N₈ ligands are extremely lengthy and time spending, due to intrinsic complexity of the polyfunctional molecules and to the fact that the synthesis must comply with the need to protect the chiral centers in every step of the procedure. We want therefore to develop a parallel, simpler approach to dinucleating N₆ ligands that would give the chance to proceed more systematically with stepwise improvements and adjustments on the basis of the performance of the resulting dicopper complexes in terms of catalytic efficiency and recognition capacity. Herein, we report the synthesis and reactivity characteristics of [Cu₂EHI]⁴⁺, the first member of a new family of chiral biomimetic tyrosinase model complexes, where the ligand EHI provides a coordination environment to each copper ion constituted by tridentate amino-bis(imidazole) residues derived from L-histidine (Scheme 1).

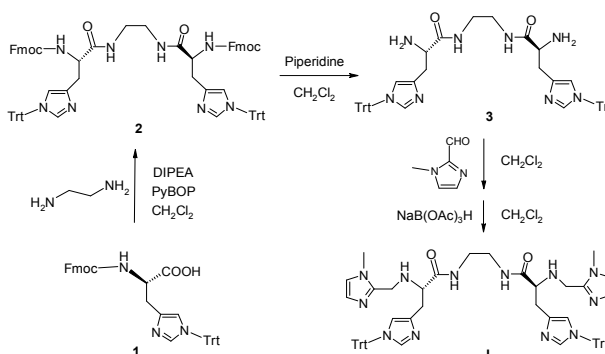


Scheme 1. Proposed structure of the dinuclear complex [Cu₂EHI]⁴⁺; Trt is the triphenylmethyl protecting group.

RESULTS AND DISCUSSION

Synthesis. The synthetic route to the diamino-tetraimidazole ligand EHI (L) is outlined in Scheme 2. It involves the preparation of Fmoc-protected bis(L-histidine) intermediate **2** by condensation of the protected amino acid **1** with ethylenediamine, followed by deprotection and condensation of the diamine **3** with two molecules of N-methyl imidazole-carboxaldehyde, and reduction of the resulting intermediate.

The dicopper(II) complex [Cu₂L]⁴⁺ was obtained by reacting the free ligand with copper(II) salt in almost quantitative yields.



Scheme 2. Synthesis of chiral diamino-tetraimidazole ligand EHI (L) from *N*-protected L-histidine. Fmoc is the fluorenylmethyloxycarbonyl protecting group.

The design of the EHI ligand features two tridentate amino-bis(imidazole) chelating arms connected through a linker chain, similarly to the previously studied ligands of the PHI family.^{11bc,12b} However, here the linker chain is built on the α -carbon atoms of L-histidine residues, whereas in the PHI ligands the linker was bound as a substituent at the nitrogen atom of the amino group. This change is important because it combines a large flexibility in ligand design with a great simplification in the synthesis of the chiral ligand.

Spectroscopic and conformational characterization of [Cu₂EHI]⁴⁺. The electronic spectrum of [Cu₂EHI]⁴⁺ (Figure 1S) in the UV region is dominated by the absorption bands of the N-trityl substituent of the histidine residues. A weak shoulder detectable on the low-energy tail of the intense UV band, near 370 nm, can be attributed to $\pi(\text{imidazole}) \rightarrow \text{Cu}(\text{II})$ LMCT transitions, as discussed previously for Cu-PHI complexes.^{11b} The visible portion of the electronic spectrum features a broad absorption band comprising the copper(II) LF transitions. The maximum occurs near 630 nm, but the band is asymmetric and extends to the near-IR. As for [Cu₂PHI]⁴⁺ complexes,^{11bc,12b} the CD spectrum of [Cu₂EHI]⁴⁺ provides important details. The visible region is dominated by a CD band of positive sign centered at 670 nm, which is flanked by a much weaker negative band at higher energy, near 550 nm (Figure 1).

Journal Name

ARTICLE

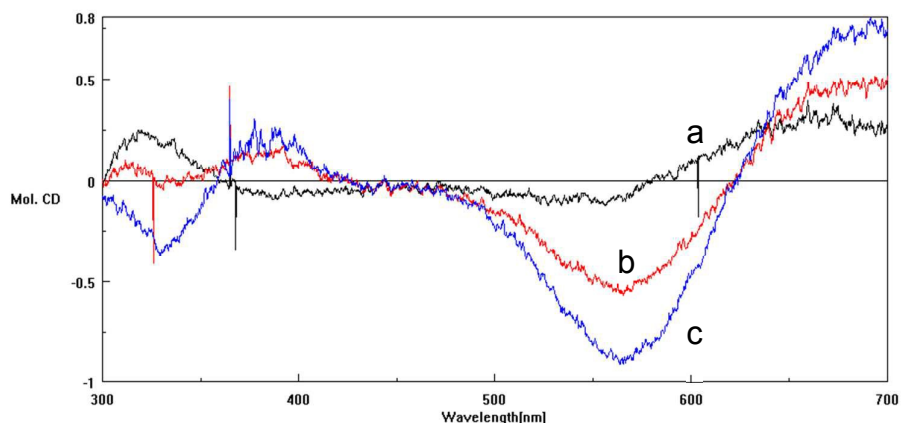
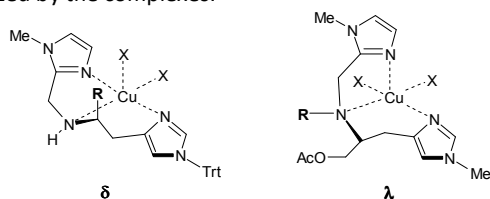


Figure 1. CD spectra in the near-UV and visible range of complex $[\text{Cu}_2\text{EHI}]^{4+}$ (a, black trace), and after the addition of 1 (b, red trace) and 2 (c, blue trace) equiv. of azide in MeOH/MeCN 9:1 (v/v) solution.

This pattern is opposite to that exhibited by Cu(II)-PHI complexes and implies a different conformational preference by the chelate ring of the L-histidine residues. This is of δ chirality for $[\text{Cu}_2\text{EHI}]^{4+}$, as shown in Scheme 3, implying that all three nitrogen donor atoms of the ligand occupy equatorial positions of Cu(II), but the preferred conformation was λ in $[\text{Cu}_2\text{PHI}]^{4+}$. The difference is dictated by the orientation of the linker chain (R in Scheme 3) attached to the histidine chelating arm, which is axial in the former case and equatorial in the latter.^{11bc,12b} In $[\text{Cu}_2\text{EHI}]^{4+}$ the R substituent on the α -carbon is more far removed from the Cu center with respect to the N-linked position it occupies in $[\text{Cu}_2\text{PHI}]^{4+}$ complexes, which forces the substituent to adopt an equatorial disposition and the chelate ring into the opposite (λ) conformational arrangement (Scheme 3). This allows the L-histidine chelate ring of $[\text{Cu}_2\text{EHI}]^{4+}$ to adopt a preferred¹³ δ conformation. These stereochemical considerations are important because they may be involved in the output of the asymmetric reactions catalyzed by the complexes.

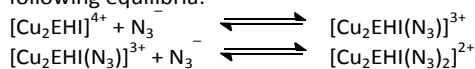


Scheme 3. Representation of the δ conformation of the L-histidine chelate ring adopted by the copper centers of $[\text{Cu}_2\text{EHI}]^{4+}$, and the λ conformation adopted by the corresponding chelate rings of $[\text{Cu}_2\text{PHI}]^{4+}$ complexes; R stands for the linker chain connecting the two halves of the dinuclear complex and X are solvent molecules or donor ligands, like azide.

Azide binding experiments to $[\text{Cu}_2\text{EHI}]^{4+}$ were performed to gain information about the mode of binding of small ligands to the copper(II) centers of the complex. The experiments were carried out in the same solvent mixture of MeOH/MeCN 9:1 (v/v) previously used for the parent $[\text{Cu}_2\text{PHI}]^{4+}$ complex to allow a direct comparison between the optical features and binding constants of the small ligand in the two complexes. The addition of azide to a solution of $[\text{Cu}_2\text{EHI}]^{4+}$ is accompanied by the development of the characteristic UV band, here near 385 nm, due to $\pi(\text{azido}) \rightarrow \text{Cu(II)}$ LMCT. The band is symmetric and grows steadily in intensity, with only a small shift in the wavelength maximum, with stepwise addition of azide up to a molar ratio of $2 \text{ N}_3 / [\text{Cu}_2\text{EHI}]^{4+}$ ($\epsilon_{382} = 4600 \text{ M}^{-1} \text{ cm}^{-1}$). A weak band of positive sign in the same position develops in the CD spectrum (Figure 1) and, together, these spectral features indicate that an azido ligand binds to each copper center of $[\text{Cu}_2\text{EHI}]^{4+}$ in the terminal mode and that the two Cu-azido chromophores are well separated in space, with negligible interaction between the LMCT transition moments. The situation is thus different from the case of $[\text{Cu}_2\text{PHI}]^{4+}$, where the spatial proximity between the two Cu-azido chromophores allowed their $\pi(\text{azido}) \rightarrow \text{Cu(II)}$ LMCT transition moments to interact, yielding a peculiar and intense exciton couplet in the CD spectrum.^{11c} In addition, while for complexes of $[\text{Cu}_2\text{PHI}]^{4+}$ type azide binding produced an inversion of the conformation of the L-histidine chelate ring, from λ to δ ,^{11c,12b} in the case of $[\text{Cu}_2\text{EHI}]^{4+}$ the ligand strengthens the optical activity of the LF bands without changing their sign (Figure 1), indicating that the δ conformation is maintained.

By optical titration it was possible to separate the two steps of azide binding to $[\text{Cu}_2\text{EHI}]^{4+}$ (Figure 2S). Analysis of the spectral

data using a non-linear least-squares procedure, enabled to estimate two binding constants, corresponding to the following equilibria:



The equilibrium constants were determined as $\log K_{b1} = 4.61 \pm 0.01$ and $\log K_{b2} = 3.59 \pm 0.01$. These values are in the same range as those for azide binding to $[\text{Cu}_2\text{PHI}]^{4+}$ complex,^{11c} and indicate moderate affinity of copper(II) centers with similar ligand environment for the exogenous ligand.

Magnetic coupling in $[\text{Cu}_2(\text{EHI})]^{4+}$. Magnetic susceptibility measurements can give information about the presence of coupling of magnetic moments in dinuclear complexes. NMR spectra can give indication about the existence of magnetic coupling and indeed the $^1\text{H-NMR}$ spectra of $[\text{Cu}_2(\text{EHI})]^{4+}$ show temperature dependence (Figure 3S). However, as signal assignment is difficult without a thorough analysis we preferred to obtain information on the nature of the coupling through the Evans method. Measurements of magnetic susceptibility on $[\text{Cu}_2(\text{EHI})]^{4+}$ were then performed in deuterated methanol/acetate buffer (50 mM, pH = 5.1) 10:1 v/v, to replicate the conditions to be used in the study of catalytic oxidations. Acetone was chosen as internal standard and added in 10 % (v/v), a concentration much larger than the paramagnetic substance. Figure 2 shows that temperature variation has a strong effect in both position and signal shape, but the most interesting parameter is the shift between the acetone signal of the solution in the absence and presence of $[\text{Cu}_2(\text{EHI})]^{4+}$. In the latter solution, the acetone signal is affected by interaction with the paramagnetic compound. This causes a low-field shift of the signal with respect to the reference signal. The analysis was performed in the

temperature range between -15 and +45 °C, as the mixture is stable in these conditions.

Table 1. Paramagnetic shift of the reference NMR signal (in Hz), magnetic susceptibility, and magnetic moment (per copper) determined at different temperatures for $[\text{Cu}_2(\text{EHI})]^{4+}$.

Temperature (K)	$\Delta\nu$ (Hz)	χ_M (m^3/mol)	μ (μ_B)
258	18.04	1.64×10^{-8}	1.64
273	15.98	1.45×10^{-8}	1.59
288	14.15	1.28×10^{-8}	1.54
301	11.94	1.08×10^{-8}	1.44
318	10.90	0.99×10^{-8}	1.42

The data in Table 1 show that the magnetic moment (per Cu) appreciably decreases with increasing temperature, which suggests the presence of a weak ferromagnetic interaction. The μ value is slightly reduced from the spin-only value due to population of the singlet excited state of the dimer. Ferromagnetic coupling is much less frequent in dinuclear copper(II) complexes than the antiferromagnetic behavior usually observed.¹⁴ We actually suspect that in the present case the weak interaction, probably mediated by a solvent molecule, occurs intermolecularly, because the rigidity of the bis-amide linker that connects the two tridentate chelating arms and the steric hindrance of the trityl substituent groups are expected to hinder the close approach of the two copper(II) centers within the same molecule. Support to this interpretation comes from the catalytic experiments described below. On the other hand, we did not observe appreciable temperature or concentration dependence in the electronic spectra of the complex.

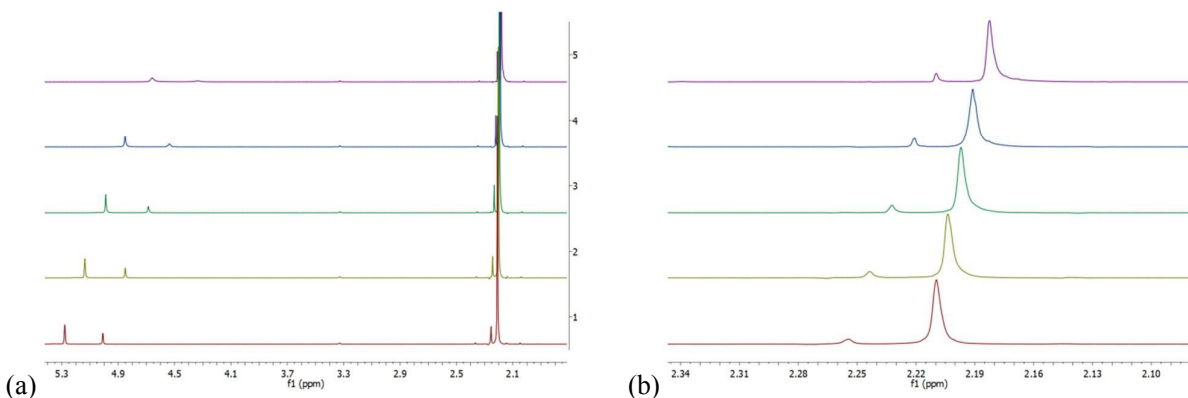
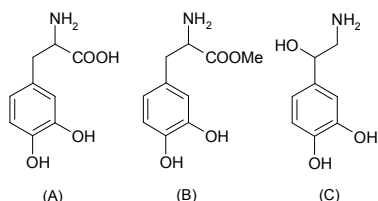


Figure 2. (a) $^1\text{H-NMR}$ spectra collected at increasing temperature (from -15 to +45 °C) of $[\text{Cu}_2(\text{EHI})]^{4+}$ in deuterated methanol/acetate buffer (pH 5.1, 50 mM) 10:1 (v/v), containing 10 % (v/v) acetone as reference compound; (b) Magnification of the range centered on acetone signal near 2.2 ppm. 1: -15 °C; 2: 0 °C; 3: 15 °C; 4: 28 °C; 5: 45 °C.

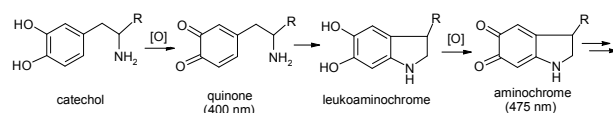
Kinetic experiments of catechol oxidation. The oxidation of a set of chiral biogenic catechols, L-/D-Dopa, the corresponding methyl esters L-/D-DopaOMe, and R-/S-norepinephrine (Scheme 4), was studied through the increase of the absorption band near 475 nm due to the formation of the

corresponding aminochromes. The latter are relatively stable intermediates produced by cyclization of the initially formed quinone, which undergo further oxidation and oligomerization reactions (Scheme 5).¹⁵ Therefore, aminochromes are suitable compounds for the determination of initial rates of the

reactions. As solutions of catecholic substrates revealed relatively high air instability when the pH was greater than 7, the rate dependence of catechol oxidation catalyzed by $[\text{Cu}_2\text{EHL}]^{4+}$ was determined at pH 5.1, even though in this pH range the catalytic efficiency of the complex is significantly reduced. However, the catecholic substrates do not undergo appreciable autoxidation by air oxygen up to pH 6, so that in these experimental conditions there is no need to subtract the contribution of non-catalytic reaction.



Scheme 4. Structure of the chiral catechol substrates: (A) Dopa, (B) DopaOMe, (C) norepinephrine.



Scheme 5. Oxidation pathway of catecholamine derivatives; the aminochrome is the only observable intermediate in normal conditions.

The rate dependence on substrate concentration was thus studied by keeping the catalyst concentration constant at 1.0 μM and varying that of substrate between 0.05 mM and 1.0 mM. For the oxidation of L-/D-Dopa and L-/D-DopaOMe (Figure 4S), the plots of the initial rates exhibited a hyperbolic behavior and the kinetic parameters (k_{cat} , K_M) could be determined using simple Michaelis–Menten treatment. This enables to consider a simplified reaction scheme implying fast initial copper(II) reduction by one molecule of catechol, followed by a complex series of events involving pre-equilibrium binding of a second catechol molecule and dioxygen to the dicopper(I) species and, finally, substrate oxidation and irreversible release of quinone product.

The plots clearly show a negligible enantiodifferentiation for L-/D-Dopa and only a modest preference for the L-enantiomer of DopaOMe (Figure 4S). The enantioselectivity indexes R_{k_{cat}/K_M} and $R_{k_{\text{cat}}}$, expressed as percentages, are used as useful parameters to evaluate the discriminating effect observed in the catalytic oxidations at low and saturating substrate concentration, respectively:¹⁷

$$R_{k_{\text{cat}}/K_M} \% = \frac{(k_{\text{cat}}/K_M)_L - (k_{\text{cat}}/K_M)_D}{(k_{\text{cat}}/K_M)_L + (k_{\text{cat}}/K_M)_D} \times 100$$

$$R_{k_{\text{cat}}} \% = \frac{(k_{\text{cat}})_L - (k_{\text{cat}})_D}{(k_{\text{cat}})_L + (k_{\text{cat}})_D} \times 100$$

For R-/S-norepinephrine the plots display a sigmoidal behavior (Figure 4S), which suggests the presence of a mechanism of substrate activation, through cooperative binding. The following equation (for derivation see Supplementary Information) was therefore used to extrapolate the kinetic parameters from the experimental data (S =substrate):

$$\frac{v}{[\text{catalyst}]} = \frac{k_{\text{cat}} [S]^2}{K' + [S]^2}$$

This behavior can be explained by considering that the binding of the first molecule of substrate results in an altered affinity or increase in the rate of product formation for a second molecule of substrate. It is difficult to hypothesize the mechanism of this effect, however we note that for an efficient catechol oxidation, the substrate should be bound as a bridging ligand to the dicopper(II) center.¹⁰ In the latter equation, K' is a constant comprising the interaction factors leading to the complex bound to two substrate molecules and has no longer the meaning, nor the units, of K_M . A comparison of the two constants is inappropriate, and therefore the enantiodifferentiating potential of the complex against the two norepinephrine enantiomers was evaluated as a ratio between the oxidation rate of the two isomers (v_R/v_S) at low (0.015 mM) and high (0.8 mM) substrate concentrations, respectively. The comparison of the kinetic parameters, summarized in Table 2, reveals that the oxidation of L-/D-Dopa occurs with the highest rate among the series of substrates, with k_{cat} values almost one order of magnitude larger than the other catechols. This result is unusual among the reactions catalyzed by chiral dinuclear complexes studied before,^{12,16} for which the reactivity is larger for DopaOMe. On the other hand, chiral recognition of L-/D-Dopa is almost negligible. For Dopa substrates, it is likely that an unproductive binding occurs to a single copper(II) center of $[\text{Cu}_2\text{EHL}]^{4+}$, through the amino and carboxylate groups. The reaction then probably occurs with negligible recognition on a second substrate molecule binding through the catecholato residue.

Journal Name

ARTICLE

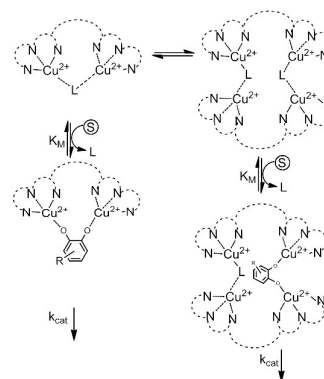
Table 2. Kinetic parameters for the enantioselective oxidation of L-/D-Dopa, L-/D-DopaOMe and R/S-norepinephrine at pH 5.1 and 20 °C, using 1.0 and 5.0 μM concentrations of [Cu₂EHI]⁴⁺.

	K _M (mM)	k _{cat} (s ⁻¹)	K' (mM ²)	R _{kcat} /K _M %	R _{kcat} %
[Cu ₂ EHI] ⁴⁺ / 1.0 μM					
L-Dopa	(2.10±0.58)×10 ⁻¹	(9.93±0.96)×10 ⁻³	-	-1	-4
D-Dopa	(2.22±0.56)×10 ⁻¹	(1.08±0.09)×10 ⁻²	-		
L-DopaOMe	(2.52±0.29)×10 ⁻¹	(1.99±0.08)×10 ⁻³	-	+15	+14
D-DopaOMe	(2.55±0.52)×10 ⁻¹	(1.50±0.11)×10 ⁻³	-		
R-norepinephrine	-	(2.84±0.01)×10 ⁻³	(4.15±0.01)×10 ⁻²	1.2 ^{a,c}	1.2 ^{b,c}
S-norepinephrine	-	(3.32±0.09)×10 ⁻³	(4.15±0.59)×10 ⁻²		
[Cu ₂ EHI] ⁴⁺ / 5.0 μM					
L-Dopa	(6.89±2.63)×10 ⁻¹	(1.68±0.36)×10 ⁻³	-	~0	+14
D-Dopa	(5.18±0.82)×10 ⁻¹	(1.27±0.09)×10 ⁻³	-		
L-DopaOMe	(3.89±0.01)×10 ⁻²	(5.36±0.01)×10 ⁻⁴	-	12.8 ^{a,c}	0.9 ^{b,c}
D-DopaOMe	-	(6.05±0.01)×10 ⁻⁴	(6.63±0.01)×10 ⁻²		
R-norepinephrine	(2.57±0.56)×10 ⁻¹	(4.07±0.31)×10 ⁻⁴	-	+3	-10
S-norepinephrine	(3.34±0.75)×10 ⁻¹	(4.98±0.39)×10 ⁻⁴	-		

^a Ratio of v_R/v_S at low [S], corresponding to the ratio between the oxidation rate for the R and S enantiomers extrapolated at the substrate concentration of 0.015 mM. ^b Ratio of v_R/v_S at high [S], corresponding to the ratio of the two oxidation rates, extrapolated at the substrate concentration of 0.8 mM. ^c Values of v_R/v_S ratio above 1.0 suggest a preference for the R enantiomer of norepinephrine, whereas for values of this ratio lower than 1.0 the discrimination favors the opposite enantiomer.

Surprisingly, when the catalytic oxidations were studied at a larger concentration (5.0 μM) of [Cu₂EHI]⁴⁺, the reaction rates significantly dropped, with k_{cat} almost one order of magnitude smaller (Table 2). In addition, in these conditions, the sigmoidal behavior was observed only for the oxidation of D-DopaOMe (Figure 5S), which suggests a peculiar interaction of this particular substrate with the chiral complex. The marked decrease in the oxidation rates suggests the existence of different forms of the complex when the concentration is changed. We assume that, for concentrations of 5 μM, or higher, the active form of the complex in the catalytic reaction could be better represented by a dimeric species, that could be promoted, for instance, by an intermolecular bridge formed by a water molecule or hydroxo group (Scheme 6). The two-electron transfer by the substrate to the dicopper(II) center occurs intermolecularly, after the substrate displaced the bridging ligand to activate the catalytic site. This step is not contemplated at lower complex concentrations (1 μM), when

the more reactive monomeric form of the dinuclear complex is present (Figure 3).

**Scheme 6.** Hypothesis on the formation of a dimeric species of the complex and its involvement in catalysis (L: solvent molecule; S: catecholic substrate).

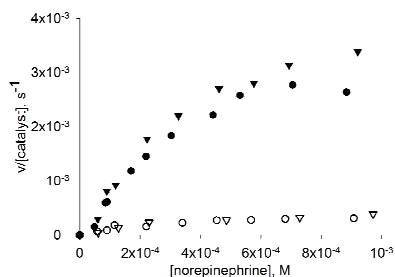


Figure 3. Effect of catalyst concentration on the initial rates of air oxidation of the enantiomers of norepinephrine by $[\text{Cu}_2(\text{EHI})]^{4+}$ studied at pH 5.1 (black symbols: $[\text{Cu}_2(\text{EHI})]^{4+} = 1 \mu\text{M}$; empty symbols: $[\text{Cu}_2(\text{EHI})]^{4+} = 5 \mu\text{M}$).

To probe the hypothesis of an involvement of a dimeric form of the complex, the oxidation of L-DopaOMe was studied as a function of $[\text{Cu}_2(\text{EHI})]^{4+}$ concentration. These experiments were carried out using a substrate concentration of 0.5 mM and varying the catalyst concentration between 5×10^{-7} and 1×10^{-5} M. As shown by the plots shown in Figure 4, as the $[\text{Cu}_2(\text{EHI})]^{4+}$ concentration increases, the rate constant decreases exponentially, indicating a quadratic dependence on catalyst concentration (see Supporting Information for derivation of the kinetic equation).

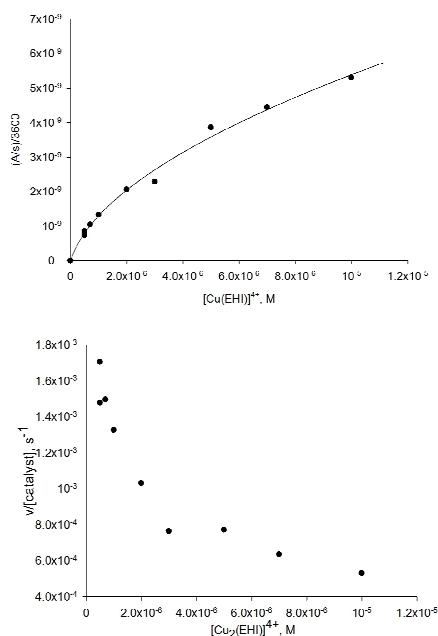


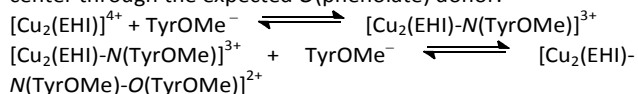
Figure 4. Dependence of the oxidation rate of L-DopaOMe on the concentration of $[\text{Cu}_2(\text{EHI})]^{4+}$. Upper plot: Rate data are expressed as Absorbance/time (A/s) units divided for $\epsilon_{\text{aminochrome}}$. Bottom plot: Rate data expressed as $(\text{A/s})/3600/[\text{Cu}_2(\text{EHI})]^{4+}$.

Even if less catalytically efficient, the dimeric form exhibits a remarkable enantioselectivity in the oxidation of DopaOMe substrates, with a strong preference for the L-enantiomer, by a

factor of almost 13 (Table 2). This corresponds to >90% ee and appears to be the highest ee so far reported for this type of reaction by any biomimetic copper complex. Surprisingly, though, the enantioselectivity progressively decreases at higher substrate concentrations, which suggests that the binding of L-DopaOMe to dimeric $[\text{Cu}_2(\text{EHI})]^{4+}$, although sterically favored, gives rise to an adduct characterized by a slower electron transfer rate with respect to the opposite D-enantiomer. This can only depend on the less favorable spatial arrangement of the orbitals of the ternary Cu^{II} -catecholate- Cu^{II} complex involved in the electron transfer process.

Binding of L-/D-tyrosine methyl ester to $[\text{Cu}_2(\text{EHI})]^{4+}$. To gain information about the difference in coordination affinity of chiral catecholic and phenolic substrates, we investigated the binding behavior of the L-/D-enantiomers of tyrosine methyl ester to $[\text{Cu}_2(\text{EHI})]^{4+}$, using their phenolate salts to improve their coordination through the phenolate oxygen donor. To prevent solubility problems, the spectrophotometric titration was carried out in methanol solution and using the diazabicycloundecene (DBU) salt of the tyrosine derivatives, as described in the Experimental Section. The optical titration experiments are shown in Figure 5.

Upon addition of tyrosine methyl ester salts, the growth of an absorption band near 430 nm is observed, which is attributable to a LMCT band from the phenolate to the copper(II) ions.¹⁸ The coordination of the tyrosinate ligand to the dicopper complex also causes a blue shift of the d-d band to about 600 nm. By processing the spectrophotometric data with a non linear least-square procedure, the ligand binding process is explained as the sequence of two steps, according to which both a 1:1 and 2:1 tyrosinate adducts of $[\text{Cu}_2(\text{EHI})]^{4+}$ are formed (Figure 6). Even though the model is simplified, as more species may be present in solution, the calculated spectra for the 1:1 and 2:1 adducts are very informative, because in the first step it is clear that binding of the tyrosinate ion to $[\text{Cu}_2(\text{EHI})]^{4+}$ does not involve ligation through the phenolate group, which does only occur in the second step. We then hypothesize that the first tyrosinate ligand (TyrOMe^-) binds to one of the copper(II) centers through the amino group, and only the second one to the other copper(II) center through the expected *O*(phenolate) donor:



Even though we could not calculate reliable binding constants for the various types of adducts, it is clear from the plots in Figure 6, that formation of the 1:2 $[\text{Cu}_2(\text{EHI})(\text{tyrosinate})_2]^{2+}$ complex occurs at lower ligand concentration for L-tyrosine methyl ester than for D-tyrosine methyl ester and hence the affinity of $[\text{Cu}_2(\text{EHI})]^{4+}$ for the L-tyrosinate ligand is higher than for D-tyrosinate isomer, in agreement with the behavior of the corresponding chiral catechols.

Journal Name

ARTICLE

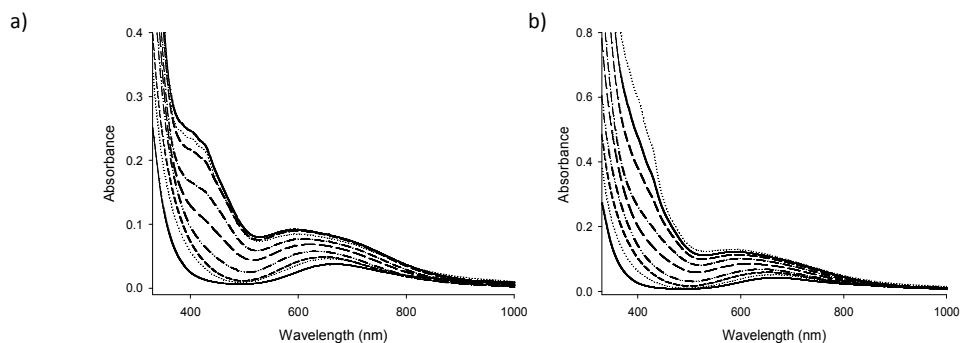


Figure 5. UV-Vis spectra recorded upon titration of $[\text{Cu}_2(\text{EHI})]^{4+}$ (5×10^{-4} M) in methanol solution with the DBU salt of L-tyrosine methyl ester (a) and D-tyrosine methyl ester (b), from 0:1 to 10:1 [tyrosinate]: $[\text{Cu}_2]$ molar ratios. The spectra were recorded at 25 ± 0.1 °C.

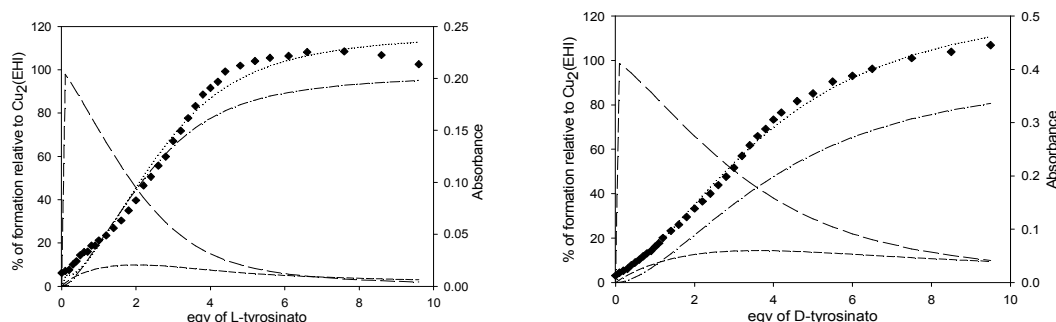
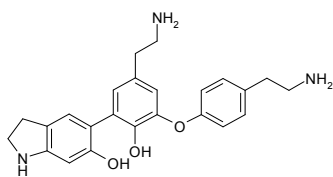


Figure 6. Absorbance profile at 428 nm during the titration of $[\text{Cu}_2(\text{EHI})]^{4+}$ with methyl L-tyrosinate (left) and methyl D-tyrosinate (right), superimposed to species distribution diagram. Diamonds: experimental absorbance values; dotted line: calculated absorbance; long dashed line: distribution of free $[\text{Cu}_2(\text{EHI})]^{4+}$; short dashed line: distribution of the 1:1 $[\text{Cu}_2(\text{EHI})\text{-tyrosinate}]^{3+}$ complex; dashed and dotted line: distribution of the 1:2 $[\text{Cu}_2(\text{EHI})(\text{tyrosinate})_2]^{2+}$ complex.

Hydroxylation of *N*-acetyl-L/D-tyrosine ethyl ester. The hydroxylation of tyrosine, and other phenolic substrates, is the most important activity of tyrosinase.¹⁹ The enzyme exhibits a marked preference for L-tyrosine than for D-tyrosine, and also for L-Dopa vs. D-Dopa,²⁰ and the difference depends exclusively on K_M . It was therefore interesting to investigate the oxidation of the two enantiomers of tyrosine by the dicopper-EHI complex. As the phenol hydroxylation is much slower than catechol oxidation, here the problem of the high reactivity of the quinone is more dramatic than before. Therefore, these experiments were performed using the tetrabutylammonium salt of *N*-acetyl L-/D-tyrosine ethyl esters, to prevent cyclization to aminochrome and trying to slow down the reactivity of the quinone. As the dicopper(II) form of the complex is not competent in the phenol hydroxylation,^{10,19} the reactions were carried out by preparing the dicopper(I) complex, $[\text{Cu}_2(\text{EHI})]^{2+}$, anaerobically, at -80 °C in dry acetone and adding an excess of the phenolate substrate

(20 equiv.) followed by exposure to air oxygen. We also tried in several attempts, albeit unsuccessfully, to characterize a copper/dioxygen adduct in various organic solvents at low temperature (down to -80 °C in dry acetone, -90 °C in dry dichloromethane, -120 °C in dry 2-methyl tetrahydrofuran). The Cu_2O_2 complex does not accumulate because as soon as it forms it reacts with dicopper(I), and for this reason exposure to O_2 of the reaction solution was always allowed after adding the phenolic substrate to $[\text{Cu}_2(\text{EHI})]^{2+}$. In any case, the color of the solution turns brown, indicating that the reaction occurs, and we made several attempts trying to isolate and characterize the oxidation products. However, the material isolated after work-up is probably a mixture of oligomeric products. The high reactivity of quinones towards nucleophiles is well known also for the enzymatic reaction.²¹ We could actually separate a main product of the reaction by chromatography and tried to characterize it by NMR and MS (Figure 6S-8S). The MS data (405 a.m.u.) and the pattern of

NMR signals would be in agreement with the following trimeric structure (or some isomeric structure):



which appears to derive from C-C and C-O radical coupling reactions of phenolic rings, decarboxylation and cyclization of one free amino group of the side chains, after deacetylation.

As a main scope of the present investigation is to assess the enantiodiscriminating properties of the dicopper-EHI system, we monitored the oxidation of the enantiomeric L-/D-tyrosine derivatives spectrophotometrically, after exposing to air a solution of $[\text{Cu}_2(\text{EHI})]^{2+}$ and excess phenolate salts of *N*-protected tyrosine ethyl esters (20 equiv.) initially prepared anaerobically. In the initial part of the reaction, a broad absorption band centered around 400 nm, attributable to some quinone product(s), increases with time (Figure 7 and 9S). The time profile of this band clearly shows a steeper increase for the L-tyrosinate substrate with respect to the D enantiomeric counterpart, indicating a faster reaction. The initial rates, in $\Delta\text{absorbance}/\text{s}$ units, are in fact 7.4×10^{-5} for ethyl *N*-acetyl-L-tyrosinate and 3.4×10^{-5} for ethyl *N*-acetyl-D-tyrosinate, that is in line with the binding preference for the L-tyrosinate ligand with respect to D-tyrosinate by $[\text{Cu}_2(\text{EHI})]^{4+}$.

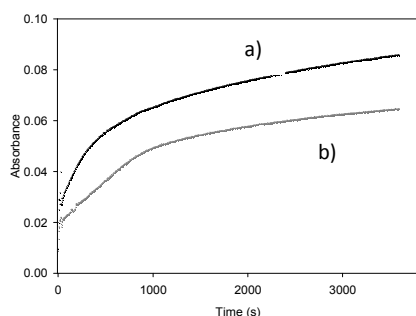
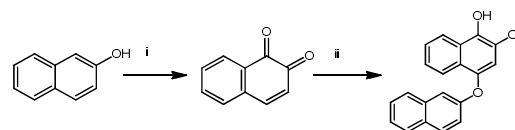


Figure 7. Time profile of the absorption at 400 nm during the oxidation of the tetrabutylammonium salts of ethyl *N*-acetyl-L-tyrosinate (a) and ethyl *N*-acetyl-D-tyrosinate (b) by $[\text{Cu}_2(\text{EHI})]^{2+}/\text{O}_2$ in acetone solution at 25 °C.

Hydroxylation of β -naphthol. In order to probe the capability of the $[\text{Cu}_2(\text{EHI})]^{2+}/\text{O}_2$ system to perform phenol hydroxylation, we used a hydrophobic substrate, β -naphthol, that could enable a easier separation and characterization of the product. The reaction was carried out using an excess of DBU salt of β -naphthol and $[\text{Cu}_2(\text{EHI})]^{2+}$ in degassed acetone, upon exposure to air at room temperature. The color of the solution turned visually from colorless to pale gold yellow and the reaction was allowed to proceed for several hours. The product of the reaction could be separated by conventional chromatography from the excess unreacted phenolate, and was identified as the regioselective conjugate addition product of β -naphthol to the initially formed 1,2-naphthoquinone, as outlined in the

reaction Scheme 7. Labeling experiments with $^{18}\text{O}_2$ showed complete absence of 18-O atom into the product, which suggests that also the naphthol hydroxylation reaction, as tyrosine oxidation, likely occurs through a radical mechanism.



Scheme 7. The steps involved in the hydroxylation of β -naphthol (as DBU salt) by $[\text{Cu}_2(\text{EHI})]^{2+}/\text{O}_2$, with the subsequent addition of β -naphtholate to the naphthoquinone product of the monooxygenase reaction.

Conclusion. The dinucleating N_6 ligand EHI, obtained through a relatively easy synthetic approach, represents the first member of a new family of chiral hexadentate ligands with potential applications in stereoselective catalysis. The different type of linkage of the two tridentate coordinating units with respect to the previous ligands of the PHI family,^{11,12b} appears to be advantageous in terms of stereochemical rigidity of the chelating rings, which are not inverted by the binding of exogenous ligands such as azide. Apparently, the opposite conformational preference of the chelate rings of $[\text{Cu}_2\text{EHI}]^{4+}$ with respect to copper-PHI type complexes^{11,12b} does not change the binding preference toward L-Dopa vs. D-Dopa and L-tyrosine vs. D-tyrosine derivatives. However, while the enantioselectivity effects in the catalytic oxidations of catechols performed with copper-PHI complexes were entirely due to the L-/D binding discrimination, for $[\text{Cu}_2\text{EHI}]^{4+}$ marked differences occur in the electron transfer step, indicating a differential orientation of the aromatic ring of the bound enantiomeric substrates with respect to the catalytic center.

Although we were unable to obtain a full structural characterization of $[\text{Cu}_2\text{EHI}]^{4+}$, because we could not obtain suitable crystals, the catecholase experiments clearly indicate that the current limit of the EHI structure is in the relatively rigid ethanediamide moiety connecting the tridentate binding units, which makes easier an intermolecular binding of the catechol substrates at relatively low concentration. The presence of equilibria between monomeric and dimeric forms of the dinuclear complexes complicates a full understanding of the catalytic reactions. However, it is worthy of note that the chiral discrimination capacity of $[\text{Cu}_2\text{EHI}]^{4+}$ towards catecholic substrates, in the best conditions, favorably compares with that of the large family of dicopper complexes with related chiral ligands studied before. High enantioselectivity has been observed in particular for the oxidation of R-/S-norepinephrine isomers, which usually occurs with poor discriminating behavior, probably because of the benzylic position of the chiral center. Work is currently in progress to replace the ethanediamide linker of EHI with longer and more flexible residues to make intramolecular cooperation between the two metal centers easier. This should enable to obtain dicopper complexes with genuine monooxygenase activity against phenolic substrates, which for the present dicopper-EHI complex occurs through a non-biomimetic radical mechanism.

Experimental Section

General considerations. All preparations were carried out using standard Schlenk techniques under an inert atmosphere of N₂ unless otherwise stated. Solvents were dried over standard drying agents and stored over 3-Å molecular sieves. All starting materials were of reagent grade and purchased from either Sigma-Aldrich Chemical Co. or VWR International and used without further purification. *N*_α-Fmoc-*N*(Im)-trityl-L-histidine (**1**) was purchased from Novabiochem, and used without further purification. Optical purity of the final ligand EHI was determined via HPLC using a Jasco HPLC instrument equipped with two PU-1580 pumps and a MD-1510 diode array detector (working range: 195–659 nm) with a chiral column Lux 5u Cellulose-1 (0.46×25 cm), eluent: hexane:2-propanol = 85:15, flow rate: 0.8 ml min⁻¹.

Elemental analyses were obtained at the Microanalysis service of the Milano Chemistry Department. CD spectra were obtained with a Jasco J500 spectropolarimeter; the spectra were recorded at 0.2 nm resolution in the range between 300 and 700 nm at 50 nm min⁻¹ with three scans acquired for each spectrum. NMR spectra were recorded with a Bruker AVANCE 400 spectrometer operating at 9.37 T with frequencies of 400.13 and 100.6 MHz for ¹H and ¹³C NMR, respectively. The data acquisition and processing were performed with a standard Bruker software package (Topspin 1.3). The UV/Vis spectra were recorded with an Agilent 8453 spectrophotometer. Mass spectra were recorded with a Thermo-Finnigan LCQ 371 ADV MAX spectrometer.

Synthesis of bis[(9H-fluoren-9-yl)methyl]-[(2S,2'S)-(ethane-1,2-diyl-bis(azanediyl))bis[1-oxo-3-(1-trityl-1H-imidazol-4-yl)propane-2,1-diyl]]dicarbamate (2**).** *N*_α-Fmoc-*N*(Im)-trityl-L-histidine (2.00 g, 3.2 mmol) was suspended in dichloromethane (8 mL) and (benzotriazol-1-yloxy)-tripyrrolidinophosphoniumhexafluorophosphate (PyBOP) (1.66 g, 3.2 mmol) was poured into the solution. Ethylenediamine (108 μL, 1.6 mmol) was added to the solution and, finally, *N,N*-diisopropylethylamine (DIPEA, 2.2 mL, 12.8 mmol) was further added as a base. The reaction mixture was stirred for 3 h at room temperature. Then, the solvent was rotary-evaporated, yielding a highly viscous colorless oil, which was purified by silica chromatography using a mixture of dichloromethane-methanol (from 98:2 to 0:100, v/v) as eluent. A white foamy solid product (2.57 g, quantitative yield) was obtained, after treatment with diethyl ether. ¹H NMR (400 MHz, CDCl₃, 298 K): δ 9.72, (br, s), δ 7.75 (d, J = 7.0 Hz, 2H), δ 7.73 (d, J = 7.0 Hz, 2H), 7.55 (d, J = 7.0 Hz, 2H), 7.47 (d, J = 8.0 Hz, 2H), 7.44–7.30 (m, 24H), 7.25 (d, J = 7.0 Hz, 2H), 7.23 (d, J = 7.0 Hz, 2H), 7.19–7.11 (m, 12H), δ 7.01 (dd, 2H), 6.64 (s, 2H), 6.04 (d, J = 6.0 Hz, 1H), 4.53–4.44 (m, 2H), 4.33–4.06 (m, 6H), 3.5 (dd, 2H), 3.41 (d, J = 13.4 Hz, 2H). ¹³C NMR (100 MHz, 298 K): δ 170 (Q); 156 (Q), 144 (Q), 142 (Q), 138 (CH), 135 (Q), 130 (CH), 128,5 (CH), 125,6 (CH), 120, 8 (CH), 120,31 (CH), 76 (Q), 67 (CH₂), 53.5 (CH), 47.5 (CH), 38 (CH₂), 31 (CH₂). MS (ESI): m/z +1263 [M+H⁺], +1285 [M+Na⁺], +1302 [M+K⁺].

Synthesis of (2S,2'S)-N,N'-(ethane-1,2-diyl)bis(2-amino-3-(1-trityl-1H-imidazol-4-yl)-propanamide) (3**).** Piperidine (2 ml, 20

mmol) was added to a solution of **2** (1.57 g, 1.2 mmol) in dichloromethane (10 ml). After stirring for 1.5 h at room temperature, the solvent was rotary-evaporated giving a yellow oil, which was washed with diethyl ether, affording a highly hygroscopic white powder (1.01 g, nearly quantitative yield). ¹H NMR (400 MHz, CDCl₃): δ 7.93–7.82 (s, 2H), 7.43–7.30 (m, 20H), 7.20–7.06 (m, 12H), 6.65 (s, 2H), 3.66–3.56 (m, 2H), 3.43–3.30 (m, 2H), 3.31–3.20 (m, 2H), 2.96 (dd, J = 14.4, 3.9 Hz, 2H), 2.75 (dd, J = 14.4, 8.0 Hz, 2H). MS (ESI): m/z +819 [M+H⁺].

Synthesis of (2S,2'S)-N,N'-(ethane-1,2-diyl)bis(2-((1-methyl-1H-imidazol-4-ylmethyl)-amino)-3-(1-trityl-1H-imidazol-4-yl)propanamide) (EHI). Compound **3** (612 mg, 0.75 mmol) was dissolved in dichloromethane (10 mL) under an inert atmosphere. A solution of 1-methyl-2-imidazole carboxaldehyde (230 mg, 2.09 mmol) in dichloromethane (1.5 mL) was slowly added. The reaction was stirred for 2 h at room temperature. The acid labile diimine could not be visualized by TLC, so the reaction was monitored by ESI-MS. Given the predominant formation of the disubstituted product, the material was transferred directly into the reduction reaction. Solid NaB(OAc)₃H (12 equiv. in 4 portions) was added portion-wise and the suspension was stirred at room temperature for two more h. The solvent was removed and the yellow oil was purified by column chromatography on silica gel, with eluent diethyl ether-2-propanol (5:3 v/v) and an increasing amount of aqueous ammonia (from 1% to 4%), to remove the reduced imidazole-carboxaldehyde (R_f=0.86). The final product was recovered by chromatography on silica using a mixture of chloroform-methanol-aqueous ammonia (10:1:0.15 v/v) as eluent, giving EHI as a colorless oil (150 mg, 26 %). ¹H NMR (400 MHz, CDCl₃): δ 7.42–7.22 (m, 20H), 7.15–7.02 (m, 12H), 6.74 (s, 2H), 6.69 (s, 2H), 6.60 (s, 2H), 3.82–3.67 (m, 4H), 3.58 (s, 6H), 3.47–3.15 (m, 6H), 2.91 (dd, J = 14.4, 5.7 Hz, 2H), 2.78 (dd, J = 14.4, 7.3 Hz, 2H). ¹³C NMR (100 MHz): δ 174.81 (Q), 146 (Q), 138.6 (CH), 137.8 (Q), 130.11 (CH), 128,5 (CH), 126.95 (CH), 121.6 (CH), 119.9 (CH), 75.6 (Q), 62.8 (CH), 44.14 (CH₂), 39.53 (CH₂), 33.2 (CH₃), 31.95 (CH₂). MS (ESI): m/z +1007 [M+H⁺].

Synthesis of [Cu₂EHI][ClO₄]₄. The ligand EHI (50 mg, 0.05 mmol) was dissolved in methanol (800 μL) yielding a yellow solution. Then, copper(II) perchlorate hexahydrate (37 mg, 0.10 mmol) in methanol (500 μL), from a stock solution, was added dropwise. The color of the solution changed from yellow to shining green, until a green solid precipitated. The solid was recovered by filtration, washed with diethyl ether (3×1 mL) and dried in air (yield: 65%). Anal. Calcd for C₆₂H₆₂Cl₄Cu₂N₁₂O₁₈·4CH₃OH (1656.3): C 47.86, H 4.74, N 10.12; found C 47.17, H 4.34, N 9.87. ESI-MS: +1431 ([Cu₂EHI](ClO₄)₃)³⁺

Synthesis of L- and D-tyrosine methyl ester. The L- or D-tyrosine powder (100 mg, 0.552 mmol) was suspended in methanol and cooled in an ice/NaCl bath. Then, SOCl₂ (1.49 mmol) was slowly added under stirring and the solution was brought to room temperature and stirred overnight. The solvent was removed by rotary evaporation to give the pure product.

General procedure for the synthesis of the DBU salts of phenolic substrates. The phenol was dissolved in 1 mL of methanol and an equimolar amount of diazabicycloundecene was added. The solution was stirred for 30 min at room temperature and the solvent removed by rotary evaporation, to give the pure product.

Azide Binding Studies. Titrations with azide were performed by addition of a concentrated methanolic solution of sodium azide to the solution of $[\text{Cu}_2\text{EHI}]^{4+}$ in MeOH/MeCN 9:1 (v/v). All measurements were done at 25 ± 0.1 °C and without any incubation of the mixtures, as the anion binding was found to be fast. Titration of $[\text{Cu}_2\text{EHI}]^{4+}$ (5.98×10^{-5} M) was performed by stepwise addition of equal amounts of the azide solution (1.00×10^{-3} M) from 0.1 to 2.0 [azide]: $[\text{Cu}_2]$ ratios. It was possible to separate the titration steps for $[\text{N}_3^-]:[\text{Cu}_2]$ between 0.1 and 1.0 ($\lambda_{\text{max}} = 389$ nm) and between 1.1 to 2.0 ($\lambda_{\text{max}} = 382$ nm). The spectral data were analyzed as previously described,^{12b,15} to deduce equilibrium constants and stoichiometry of formation of the adducts. CD spectra of the azide adducts were recorded after the addition of 1.0 and 2.0 equiv. of the ligand.

Determination of magnetic susceptibility and magnetic moment of $[\text{Cu}_2(\text{EHI})]^{4+}$ with the Evans method. This experiment was performed using a coaxial NMR tube containing solvent and reference compound in the presence (A) or absence (B) of the complex. Solution A was prepared as follows: 110 μL of 1 mM solution of $[\text{Cu}_2(\text{EHI})]^{4+}$ in 10:1 (v/v) deuterated methanol/acetate buffer (pH = 5.1, 50 mM) to which 10 % volume of acetone (11 μL) was added. Solution B was prepared as follows: 660 μL of 10:1 (v/v) deuterated methanol/acetate buffer (pH = 5.1, 50 mM) to which 10 % volume of acetone (66 μL) was added. Solution A was loaded into the internal tube, while solution B loaded into the outer tube. ¹H-NMR spectra were recorded at various temperatures (-15 °C, 0, 15 °C, 28 °C, 45 °C) and shifts between the acetone signals in solutions (A) and (B) were recorded.

Catalytic oxidations of o-catechols. The catecholase activity of complex $[\text{Cu}_2(\text{EHI})]^{4+}$ was determined by studying the oxidation of the chiral catechols L-Dopa, D-Dopa, L-DopaOMe, D-DopaOMe, R-(-)-norepinephrine, and S-(+)-norepinephrine. The kinetic studies were carried out spectrophotometrically by the method of initial rates by monitoring the increase of each characteristic aminochrome absorption band over time. The reading wavelengths were: 475 nm for L-/D-Dopa, 468 nm for L-/D-DopaOMe, and 480 nm for R-/S-norepinephrine. The solvent used was a 10:1 (v/v) mixture of methanol/aqueous acetate buffer (50 mM, pH 5.1), saturated with atmospheric dioxygen. To check the contribution of the autoxidation reaction of the catechols, we used the same solution without adding the catalyst as internal reference. The experiments were carried out over a substrate concentration range (from 5×10^{-5} to 1×10^{-3} M) at a constant temperature of 25 ± 0.1 °C, to determine the dependence of the rate on substrate concentration. To maintain pseudo-first order conditions, a 5×10^{-5} M solution of $[\text{Cu}_2(\text{EHI})]^{4+}$ was treated with a minimum of 10 equiv. of substrate, as the lowest concentration.

Kinetic studies of L-/D-Dopa oxidation. Two stock solutions of 8×10^{-4} M of L- and D-Dopa were prepared in a 1:1 (v/v) mixture of methanol/aqueous buffer. To favor the dissolution in the stock solution mixture, we found it useful to dissolve the substrates first in buffer solution and then in the remaining volume of methanol, with mild warming of the mixture. The exact substrate concentration was then controlled on the basis of the absorbance values measured at 283 nm, the wavelength of maximum absorbance for the catechols ($\epsilon_{\text{Dopa}} = 2700 \text{ M}^{-1} \text{ cm}^{-1}$). The kinetic measurements were performed diluting the stock substrate solution to the desired concentration; after recording the blank spectrum, the reaction was initiated by the addition of a small volume of a concentrated solution of the catalyst dissolved in methanol (final concentration 5×10^{-6} M). Absorption spectra of these solutions were recorded at a regular time interval of 1 s for 5 min in the wavelength range 200–800 nm. The reaction was followed by monitoring the increase in the absorbance at 475 nm ($\epsilon_{475} = 3600 \text{ M}^{-1} \text{ cm}^{-1}$)²² as a function of time.

Kinetic studies of L-/D-DopaOMe oxidation. These experiments were carried out following the same procedure described before. Due to their better solubility in organic solvents, the stock solutions of L- and D-DopaOMe were prepared in methanol, and their concentrations corrected on the basis of the absorbance measured at 283 nm ($\epsilon_{\text{DopaOMe}} = 2700 \text{ M}^{-1} \text{ cm}^{-1}$). The catecholase activity was followed spectrophotometrically by monitoring the increase in the absorbance at 468 nm (the ϵ value used was assumed to be the same as that of dopachrome)²² as a function of time.

Kinetic studies of R-/S-norepinephrine oxidation. Also for the oxidation of S-/R-norepinephrine L-bitartrate we followed the same general procedure described before. The initial solutions of the substrates were prepared in a 1:1 (v/v) mixture of methanol/aqueous buffer, and their concentrations corrected on the basis of the absorbance measured at 283 nm ($\epsilon_{\text{norepinephrine}} = 3070 \text{ M}^{-1} \text{ cm}^{-1}$). The catechol oxidations were followed spectrophotometrically by monitoring the increase in the absorbance at 480 nm (the ϵ value used was assumed to be the same as that of dopachrome)²² with time.

Binding of L- and D-tyrosine methyl ester to $[\text{Cu}_2\text{EHI}]^{4+}$. Spectrophotometric titration of $[\text{Cu}_2\text{EHI}]^{4+}$ (5×10^{-4} M) in methanol solution was performed by addition of successive amounts of a methanolic solution of the DBU salt of each enantiomer of tyrosine methyl ester, 0.05 M, from 0:1 to 10:1 [tyrosinate]: $[\text{Cu}_2]$ molar ratios, maintaining a constant temperature of 25 ± 0.1 °C. The spectral data were then analyzed with HypSpec,²³ considering the spectral changes in the range of wavelengths between 370 and 764 nm.

Low temperature hydroxylation of tetrabutylammonium N-acetyl-L-tyrosinate ethyl ester. An oven-dried 100 mL round bottom flask equipped with a stirring bar and a rubber septum was degassed and backfilled with Ar, then charged with anhydrous acetone (47 mL). Previously prepared solutions in dry acetone of tetrabutylammonium salt of the tyrosine derivative (1×10^{-5} mol in 1 mL) and EHI (5×10^{-7} mol in 1 mL) were cannulated into the reaction flask. The mixture was cooled at -80 °C with a cryostat and carefully degassed and

ARTICLE

Journal Name

kept under N₂. Separately, [Cu(CH₃CN)₄]PF₆ (1×10⁻⁶ mol) was dissolved in dry and degassed acetone (1 mL). This solution was cooled and added to the reaction flask, via cannula, under Ar. To the reactor was subsequently applied an O₂-filled balloon to assure an approximately constant pressure of O₂. At the end of the reaction, the vessel was opened to the atmosphere and the mixture was quenched at low temperature with 2 mL of 1 M HClO₄. The organic solvent was removed in vacuo and the aqueous phase was extracted with CH₂Cl₂ (3×10 mL). The combined organic fractions were then dried over Na₂SO₄, filtered and rotary evaporated to afford an oil which was analyzed directly by ¹H-NMR. The crude reaction mixture was purified using column chromatography using silica gel and hexane as eluent.

Hydroxylation of N-acetyl-L/D-tyrosine ethyl ester.

Spectrophotometric study. A solution of EHI (5×10⁻⁵ M) and the tetrabutylammonium salt of the tyrosine derivative (10⁻³ M) was prepared in freshly distilled and degassed acetone (2 mL) in a screw-cap thermostated optical cell, stoppered with a rubber septum. A solution of [Cu(CH₃CN)₄]PF₆ in freshly distilled and degassed acetone (10⁻⁴ M, 1 mL) was added to the previous solution, through a cannula, maintaining the mixture under an inert atmosphere. The reaction was initiated by exposure to dioxygen and followed by spectrophotometry, monitoring the increase in intensity of the broad absorption band at 400 nm during 3600 s. The comparison of the reactivity of the two tyrosine enantiomers was made through the initial rates of development of the band at 400 nm.

Hydroxylation of β-naphthol. A solution of EHI (5×10⁻⁵ M) and the DBU salt of the naphthol (1×10⁻³ M) was prepared in degassed, dry acetone (20 mL), maintaining an argon atmosphere with the use of a Schlenk line. A solution of Cu(CH₃CN)₄PF₆ in freshly distilled and degassed acetone (1×10⁻⁴ M, 1 mL) was added to the above solution, with a gas-tight syringe. The reaction was initiated by the addition of dioxygen and was stirred at room temperature overnight; the color of the solution turned from colorless to pale-gold yellow. The solvent was removed by rotary evaporation, then the crude product was dissolved in dichloromethane and a few drops of distilled water were added, followed by a small amount of the disodium salt of EDTA. The organic phase was separated and evaporated to give the crude product. Purification by liquid chromatography, using silica gel (230-400 Å mesh) and eluting with hexane/ethyl acetate 7:3 gives the final product (R_f = 0.38). ¹H NMR (400 MHz, acetone-d₆) δ 8.82 (s, 1H), 8.13 (d, J = 7.3 Hz, 1H), 7.97 (d, J = 9.0 Hz, 1H), 7.91 (d, J = 8.5 Hz, 1H), 7.77 (d, J = 7.6 Hz, 1H), 7.56 (dd, J = 11.6, 7.4 Hz, 2H), 7.44–7.21 (m, J = 7.1 Hz, 4H), 6.85 (d, J = 7.6 Hz, 1H), 6.46 (s, 1H).

Acknowledgments

This work was supported by the Italian MIUR. CIRCMSB is also gratefully acknowledged.

References

1. L. Que, Jr., W.B. Tolman, *Nature*, 2008, **455**, 333-340.

2. S. Itoh, in *Copper-Oxygen Chemistry*, K. D. Karlin, S. Itoh Eds, Wiley, Hoboken, N. J., 2011, pp.225-282.

3. M. R. Halvagar, D. J. Salmon, W. B. Tolman, In *Comprehensive Inorganic Chemistry II*, Volume 3, J. Reedijk, K. Poeppelmeier Eds., Elsevier, 2013, pp. 455-486.

4. M. Rolff, J. Schottenheim, H. Decker, F. Tuczek, *Chem. Soc. Rev.*, 2011, **40**, 4077-4098.

5. M. Rolff, J. Schottenheim, G. Peters, F. Tuczek, *Angew. Chem. Int. Ed.*, 2010, **49**, 6438-6422.

6. A. Hoffmann, C. Citek, S. Binder, A. Goos, M. Rübhausen, O. Troeppner, I. Ivanović-Burmazović, E. C. Wasinger, T. D. P. Stack, S. Herres-Pawlis, *Angew. Chem. Int. Ed.*, 2013, **52**, 5398-5401.

7. I. Gamba, S. Palavicini, E. Monzani, L. Casella, *Chem. Eur. J.* 2009, **15**, 12932-12936.

8. A. Spada, S. Palavicini, E. Monzani, L. Bubacco, L. Casella, *Dalton Trans.*, 2009, 6468-6471.

9. A. Alexakis, N. Krause, S. Woodward, Eds., *Copper-Catalyzed Asymmetric Synthesis*, Wiley-VCH, Weinheim, 2014.

10. G. Battaini, A. Granata, E. Monzani, M. Gullotti, L. Casella, *Adv. Inorg. Chem.* 2006, **58**, 185- 233.

11. (a) L. Santagostini, M. Gullotti, R. Pagliarin, E. Monzani, L. Casella, *Chem. Commun.* 2003, 2186-2187; (b) L. Santagostini, M. Gullotti, R. Pagliarin, E. Bianchi, L. Casella, E. Monzani, *Tetrahedron: Asymmetry* 1999, **10**, 281-295; (c) M. Gullotti, L. Santagostini, R. Pagliarin, S. Palavicini, L. Casella, E. Monzani, G. Zoppellaro, *Eur. J. Inorg. Chem.* 2008, 2081-2089.

12. (a) M. C. Mimmi, M. Gullotti, L. Santagostini, G. Battaini, E. Monzani, R. Pagliarin, G. Zoppellaro, L. Casella, *Dalton Trans.* 2004, 2192-2201; (b) F. G. Mutti, M. Gullotti, L. Casella, L. Santagostini, R. Pagliarin, K. Kristoffer Andersson, M. F. Iozzi, G. Zoppellaro, *Dalton Trans.* 2011, **40**, 5436-5457; (c) F. G. Mutti, G. Zoppellaro, M. Gullotti, L. Santagostini, R. Pagliarin, K. Kristoffer Andersson, L. Casella, *Eur. J. Inorg. Chem.* 2009, 554-566.

13. (a) L. Casella, M. Gullotti, *J. Inorg. Biochem.* 1983, **18**, 19-31; L. Casella, M. Gullotti, *Inorg. Chem.* 1983, **22**, 242-249; (c) L. Casella, M. Gullotti, *Inorg. Chem.* 1985, **24**, 84-88.

14. I. Bertini, C. Luchinat, "NMR of paramagnetic substances", Elsevier, Amsterdam, 1996, Chapter 5.

15. (a) J. D. Simon, D. N. Peles, *Acc. Chem. Res.* 2010, **43**, 1452-1460; (b) A. Napolitano, P. Manini, M. d'Ischia, *Curr. Med. Chem.* 2011, **18**, 1832-1845; M. d'Ischia, A. Napolitano, V. Ball, C.-T. Chen, M. J. Buehler, *Acc. Chem. Res.* 2014, **47**, 3541-3550.

16. M. L. Perrone, E. Lo Presti, S. Dell'Acqua, E. Monzani, L. Santagostini, L. Casella, *Eur. J. Inorg. Chem.* 2015, 3493-3500.

17. T. Plenge, R. Dillinger, L. Santagostini, L. Casella, F. Tuczek, *Z. Anorg. Allg. Chem.* 2003, **629**, 7381-7389.

18. (a) R. C. Holz, J. M. Bradshaw, B. Bennett, *Inorg. Chem.* 1998, **37**, 1219-1225; (b) C. Belle, C. Beguin, I. Gautier-Luneau, S. Hamman, C. Philouze, J. L. Pierre, F. Thomas, S. Torelli, *Inorg. Chem.* 2002, **41**, 479-491.

19. (a) N. Wang, D. N. Hebert, *Pigm. Cell Res.* 2006, **19**, 3-18; (b) E. I. Solomon, D. E. Heppner, E. M. Johnston, J. W. Ginsbach, J. Cirera, M. Qayyum, M. T. Kieber-Emmons, C. H. Kjaergaard, R. G. Hadt, L. Tian, *Chem. Rev.* 2014, **114**, 3659-3853.

Journal Name

ARTICLE

20. J. C. Espin, P. A. Garcia-Ruiz, J. Tudela, F. Garcia-Canovas, *Biochem. J.* 1998, **331**, 547-551.
21. (a) G. Battaini, E. Monzani, L. Casella, E. Lonardi, A. W. J. W. Tepper, G. W. Canters, L. Bubacco, *J. Biol. Chem.* 2002, **277**, 44606-44612; (b) S. M. Marino, S. Fogal, M. Bisaglia, S. Moro, G. Scartabelli, L. De Gioia, A. Spada, E. Monzani, L. Casella, S. Mammi, L. Bubacco, *Arch. Biochem. Biophys.* 2011, **505**, 67-74; (c) A. Spada, S. Palavicini, E. Monzani, L. Bubacco, L. Casella, *Dalton Trans.* 2009, 6468-6471.
22. A. Granata, E. Monzani, L. Bubacco, L. Casella, *Chem. Eur. J.* 2006, **12**, 2504-2514.
23. P. Gans, A. Sabatini, A. Vacca, *Talanta*, 1996, **43**, 1739-1753.

Graphical abstract

A new dicopper(II) complex with histidine-derived N₆ ligand performs biomimetic stereoselective oxidation of catechols.

